

Supporting information for  
*Ratcheting rotation or speedy spinning:  
EPR and dynamics of Sc<sub>3</sub>C<sub>2</sub>@C<sub>80</sub>*

Juho Roukala,<sup>a</sup> Michal Straka,<sup>b</sup> Stefan Taubert,<sup>c</sup>  
Juha Vaara,<sup>a</sup> and Perttu Lantto<sup>\*a</sup>

<sup>a</sup>NMR Research Unit, P.O. Box 3000, FI-90014 University of Oulu, Finland

<sup>b</sup>Institute of Organic Chemistry and Biochemistry, Flemingovo nam. 2,  
CZ-16610 Prague, Czech Republic

<sup>c</sup> Department of Chemistry, P.O. Box 55, FI-00014 University of Helsinki, Finland

# Contents

<b>1</b>	<b>Results</b>	<b>S3</b>
<b>2</b>	<b>Computational details</b>	<b>S12</b>
2.1	Completeness-optimised basis set for Sc . . . . .	S15
2.2	Eckart frame of Sc <sub>3</sub> . . . . .	S15
2.3	Movement of C <sub>2</sub> . . . . .	S16

# List of Tables

S1	Average $g$ and $\mathbf{A}^{\text{Sc}}$ tensors at 300 K and 100 K . . . . .	S5
S2	Average $g$ and $\mathbf{A}^{\text{Sc}}$ tensors at 100 K before Sc <sub>3</sub> reorientation . . . . .	S6
S3	Average isotropic $g$ - and $A^{\text{Sc}}$ -values at 300 K and 100 K . . . . .	S6
S4	Gaussian exponents of the scandium 21s12p10d2f basis set . . . . .	S15

# List of Figures

S1	The deviation $\Delta g$ of the isotropic $g$ -factor from the free-electron $g$ -value at $T = 300$ K and 100 K . . . . .	S7
S2	The isotropic $A^{\text{Sc}}$ -values at $T = 300$ and 100 K . . . . .	S8
S3	Relative tilt and rotation angles of the Sc <sub>3</sub> moiety at $T = 300$ K and 100 K . . . . .	S9
S4	Distances between the scandium atoms and the reference carbons of the cage at $T = 100$ K . . . . .	S10
S5	Reference carbon atoms used to calculate Sc <sub>3</sub> tilt and rotation angles . . . . .	S11
S6	Shape and orientation of the average $\mathbf{A}^{\text{Sc}}$ tensors at 100 K . . . . .	S12
S7	Shape and orientation of the average $\mathbf{A}^{\text{Sc}}$ tensors at 100 K before Sc <sub>3</sub> reorientation . . . . .	S12
S8	Temperature during the <i>NVE</i> simulation at 300 K . . . . .	S13
S9	Temperature during the <i>NVE</i> simulation at 100 K . . . . .	S14

# 1 Results

The full average  $g$  and  $\mathbf{A}^{\text{Sc}}$  tensors are listed in Table S1. Figures S1 and S2 show the variation of the isotropic values, deviation  $\Delta g$  from the free-electron  $g$ -value and the hyperfine  $A(^{45}\text{Sc})$  values, respectively, along the trajectories at 300 K and 100 K. At the higher temperature, the rotation of the metal trimer is quite free, as shown in the top panels of Figure S3. In the course of the low-temperature trajectory, the metal trimer made one jump to a new position with respect to the cage (see lower panels in Figure S3, as well as Figures S4 and S5 below). In order to see the effect of the jump on the tensors, they were averaged, besides over the entire thermalised trajectory, also over only the first 5000 snapshot calculations (see Table S2), where the trimer remains roughly locked into its initial position.

To indirectly consider the effect of the isotropic model of the EPR parameters, also isotropic  $g$ - and  $A$ -values were calculated from the average tensors at both temperatures. The  $g$ - and  $A$ -values are listed in Table S3. The time variation of  $\Delta g$  and  $A^{\text{Sc}}$ , plotted in Figures S1 and S2, shows that, while the values of the individual scandium atoms oscillate rapidly at the high temperature, the average isotropic hyperfine constant over all the three scandiums oscillates much less, which likely explains the difference between the results of the models of equivalent and inequivalent scandium atoms discussed in the article. Compared to the high-temperature trajectory, there are, at 100 K, comparatively long time ranges with well-defined, distinctly different values instead of the persistent oscillation characteristic of the 300 K simulation. The hyperfine values in Figure S2 show that one of the scandiums (*e.g.*, the inequivalent scandium at the beginning of the trajectory) clearly differs from the other two, unlike the situation at the higher temperature, which explains why the equivalent-scandium EPR spectrum differs from that appropriate to the inequivalent one.

In Ref. 1, a frozen-solution EPR spectra of the system was modeled by assuming an axially symmetric hyperfine tensor for each Sc, with the principal components  $A_{\perp} = 0$  and  $A_{\parallel} = 3A_{\text{iso}}$ . In the study, two orientations of the hyperfine tensors were tested, either perpendicular to the  $\text{Sc}_3$  plane, or parallel to it, with the former found to better, albeit not perfectly, match the experimentally measured spectrum. Because the tensor orientations are readily available from first-principles calculations, the validity of the assumption is easily tested. Figures S6 and S7 show a visual representation of the rough shape and orientation of the hyperfine tensors of each scandium, calculated from the tensors averaged both over all snapshots and only the first 5000 snapshots, respectively (in the latter again to exclude jump-like ratcheting motion of the the metal trimer).

While the jump-like motion of the  $\text{Sc}_3$  moiety is seen to slightly affect the tensor shapes, the overall result is that, during the sampled trajectory, all the  $^{45}\text{Sc}$  hyperfine tensors are almost axially symmetric, with one of the principal components clearly larger than the two others. The orientation

of the distinct principal axis is neither exactly parallel nor perpendicular to the  $\text{Sc}_3$  plane. This, however, may also be affected by the limited trajectory length where the metal trimer does not thoroughly sample all of the available phase space. In any case, contrary to the assumption made in Ref. 1, the scandium centers are not equivalent, and especially the relative size of the principal components of the distinct scandium is smaller than that of the other two Sc centers.

Table S1: Total  $g$  and  $\mathbf{A}$  tensors (in MHz) of the three  $^{45}\text{Sc}$  atoms, averaged over 12000 (at 300 K) and 9000 (100 K) evenly spaced (in 8 fs and 32 fs intervals, respectively) snapshots from microcanonical molecular dynamics trajectories, after transformation of the instantaneous tensors into the Eckart frame of the  $\text{Sc}_3$  subsystem. The standard error of mean  $s = \sigma/\sqrt{N}$  is used to estimate the error limits, where  $\sigma$  is the standard deviation and  $N$  is the number of snapshots.

$T$ (K)	Tensor		$x$	$y$	$z$
300	$\mathbf{g}$	$x$	$1.99684 \pm 0.00002$	$0.00005 \pm 0.00001$	$-0.00006 \pm 0.00001$
		$y$	$-0.00001 \pm 0.00001$	$1.99769 \pm 0.00001$	$0.00020 \pm 0.00001$
		$z$	$-0.00003 \pm 0.00001$	$0.00021 \pm 0.00001$	$1.99775 \pm 0.00001$
	$\mathbf{A}^{\text{Sc1}}$	$x$	$-22.88 \pm 0.13$	$0.05 \pm 0.08$	$0.15 \pm 0.13$
		$y$	$0.05 \pm 0.08$	$-16.90 \pm 0.09$	$6.21 \pm 0.08$
		$z$	$0.15 \pm 0.13$	$6.21 \pm 0.08$	$-9.42 \pm 0.16$
	$\mathbf{A}^{\text{Sc2}}$	$x$	$-20.65 \pm 0.11$	$0.53 \pm 0.06$	$-0.95 \pm 0.09$
		$y$	$0.53 \pm 0.06$	$-12.95 \pm 0.10$	$-5.68 \pm 0.07$
		$z$	$-0.95 \pm 0.09$	$-5.68 \pm 0.07$	$-3.76 \pm 0.16$
	$\mathbf{A}^{\text{Sc3}}$	$x$	$-19.88 \pm 0.11$	$0.82 \pm 0.12$	$-0.27 \pm 0.03$
		$y$	$0.82 \pm 0.12$	$-2.88 \pm 0.19$	$1.02 \pm 0.05$
		$z$	$-0.27 \pm 0.03$	$1.02 \pm 0.05$	$-15.89 \pm 0.09$
	$\mathbf{A}^{\text{avg}}$	$x$	$-21.14 \pm 0.09$	$0.47 \pm 0.05$	$-0.36 \pm 0.06$
		$y$	$0.47 \pm 0.05$	$-10.91 \pm 0.10$	$0.52 \pm 0.03$
		$z$	$-0.36 \pm 0.06$	$0.52 \pm 0.03$	$-9.69 \pm 0.11$
100	$\mathbf{g}$	$x$	$1.99765 \pm 0.00002$	$0.00025 \pm 0.00001$	$-0.00015 \pm 0.00001$
		$y$	$0.00022 \pm 0.00001$	$1.99735 \pm 0.00001$	$-0.00022 \pm 0.00001$
		$z$	$0.00012 \pm 0.00001$	$-0.00016 \pm 0.00001$	$1.99868 \pm 0.00001$
	$\mathbf{A}^{\text{Sc1}}$	$x$	$-21.77 \pm 0.12$	$7.40 \pm 0.11$	$8.42 \pm 0.11$
		$y$	$7.40 \pm 0.11$	$-22.99 \pm 0.08$	$3.11 \pm 0.07$
		$z$	$8.42 \pm 0.11$	$3.11 \pm 0.07$	$-16.31 \pm 0.15$
	$\mathbf{A}^{\text{Sc2}}$	$x$	$-20.43 \pm 0.14$	$-7.52 \pm 0.10$	$9.31 \pm 0.13$
		$y$	$-7.52 \pm 0.10$	$-25.40 \pm 0.05$	$-1.68 \pm 0.08$
		$z$	$9.31 \pm 0.13$	$-1.68 \pm 0.08$	$-19.12 \pm 0.17$
	$\mathbf{A}^{\text{Sc3}}$	$x$	$-17.14 \pm 0.08$	$-0.81 \pm 0.08$	$-0.07 \pm 0.04$
		$y$	$-0.81 \pm 0.08$	$-3.86 \pm 0.21$	$-0.23 \pm 0.04$
		$z$	$-0.07 \pm 0.04$	$-0.23 \pm 0.04$	$-14.66 \pm 0.07$
	$\mathbf{A}^{\text{avg}}$	$x$	$-19.78 \pm 0.10$	$-0.31 \pm 0.04$	$5.88 \pm 0.07$
		$y$	$-0.31 \pm 0.04$	$-17.42 \pm 0.07$	$0.40 \pm 0.02$
		$z$	$5.88 \pm 0.07$	$0.40 \pm 0.02$	$-16.70 \pm 0.10$

Table S2: Total  $g$  and  $\mathbf{A}$  tensors (in MHz) of the three  $^{45}\text{Sc}$  atoms at 100 K, averaged over the first 5000 evenly spaced (32 fs) snapshots from microcanonical molecular dynamics trajectories, after transformation of the instantaneous tensors into the Eckart frame of the  $\text{Sc}_3$  subsystem. The standard error of mean  $s = \sigma/\sqrt{N}$  is used to estimate the error limits, where  $\sigma$  is the standard deviation and  $N$  is the number of snapshots.

$T$ (K)	Tensor	$x$	$y$	$z$	
100	$\mathbf{g}$	$x$	$1.997649 \pm 0.000014$	$0.000250 \pm 0.000005$	$-0.000148 \pm 0.000007$
		$y$	$0.000221 \pm 0.000005$	$1.997353 \pm 0.000007$	$-0.000223 \pm 0.000003$
		$z$	$0.000120 \pm 0.000012$	$-0.000162 \pm 0.000009$	$1.998685 \pm 0.000016$
$\mathbf{A}^{\text{Sc1}}$	$x$	$-27.14 \pm 0.14$	$14.89 \pm 0.04$	$15.51 \pm 0.05$	
	$y$	$14.89 \pm 0.04$	$-25.72 \pm 0.03$	$5.06 \pm 0.08$	
	$z$	$15.51 \pm 0.05$	$5.06 \pm 0.08$	$-16.26 \pm 0.17$	
$\mathbf{A}^{\text{Sc2}}$	$x$	$-25.33 \pm 0.16$	$-14.09 \pm 0.03$	$15.83 \pm 0.05$	
	$y$	$-14.09 \pm 0.03$	$-25.12 \pm 0.04$	$-4.49 \pm 0.07$	
	$z$	$15.83 \pm 0.05$	$-4.49 \pm 0.07$	$-12.41 \pm 0.18$	
$\mathbf{A}^{\text{Sc3}}$	$x$	$-19.82 \pm 0.05$	$0.21 \pm 0.02$	$-1.81 \pm 0.02$	
	$y$	$0.21 \pm 0.02$	$7.51 \pm 0.10$	$0.39 \pm 0.05$	
	$z$	$-1.81 \pm 0.02$	$0.39 \pm 0.05$	$-11.28 \pm 0.05$	
$\mathbf{A}^{\text{avg}}$	$x$	$-24.10 \pm 0.10$	$0.34 \pm 0.02$	$9.85 \pm 0.03$	
	$y$	$0.34 \pm 0.02$	$-14.45 \pm 0.05$	$0.32 \pm 0.02$	
	$z$	$9.85 \pm 0.03$	$0.32 \pm 0.02$	$-13.32 \pm 0.12$	

Table S3: Isotropic  $g$ - and  $A$ -values of the corresponding tensors of the three  $^{45}\text{Sc}$  atoms, averaged over 12000 (at 300 K) and 9000 (100 K) evenly spaced snapshots from microcanonical molecular dynamics trajectories. The standard error of mean  $s = \sigma/\sqrt{N}$  is used to estimate the error limits, where  $\sigma$  is the standard deviation and  $N$  is the number of snapshots.

$T$ (K)	Ref.	$g_{\text{iso}}$	$A_{\text{iso}}^{\text{Sc1}}$ (MHz)	$A_{\text{iso}}^{\text{Sc2}}$ (MHz)	$A_{\text{iso}}^{\text{Sc3}}$ (MHz)	$A_{\text{iso}}^a$ (MHz)
300	This work	$1.99743 \pm 0.00001$	$-16.40 \pm 0.06$	$-12.45 \pm 0.08$	$-12.88 \pm 0.08$	$-13.91 \pm 0.08$
100	This work	$1.99790 \pm 0.00001$	$-20.36 \pm 0.06$	$-21.65 \pm 0.03$	$-11.89 \pm 0.08$	$-17.96 \pm 0.08$
100 <sup>b</sup>	This work	$1.99766 \pm 0.00001$	$-23.04 \pm 0.03$	$-20.96 \pm 0.03$	$-7.87 \pm 0.06$	$-17.29 \pm 0.06$
300 <sup>c</sup>	1	1.9976				17.52
Static <sup>d</sup>	2		-6.84	-13.92	-13.92	
Static <sup>e</sup>	2		-1.13	-9.28	-9.28	

<sup>a</sup>Average over the three Sc atoms

<sup>b</sup>First 5000 snapshots

<sup>c</sup>Experimental, in the assumed  $\text{Sc}_3@C_{82}$ . Converted with  $B/\text{mT} = 10^9 h\nu / (g\mu_B) / \text{MHz}$ .

<sup>d</sup>First-principles, static calculation with the 1a isomer.

<sup>e</sup>First-principles, static calculation with the 2a isomer.

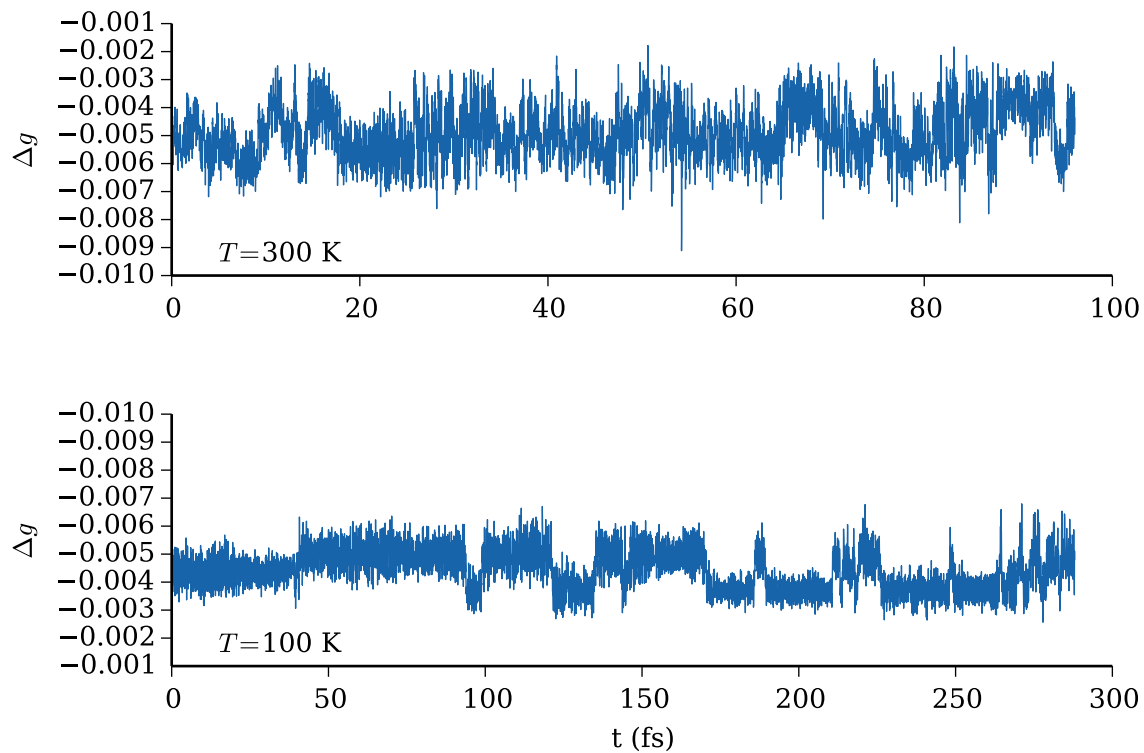


Figure S1: The deviation of the isotropic  $g$ -factor from the free-electron  $g$ -value  $g_e = 2.0023193$ ,  $\Delta g = g_{\text{iso}} - g_e$ , during the simulation at  $T = 300\text{ K}$  (top) and  $100\text{ K}$  (bottom).

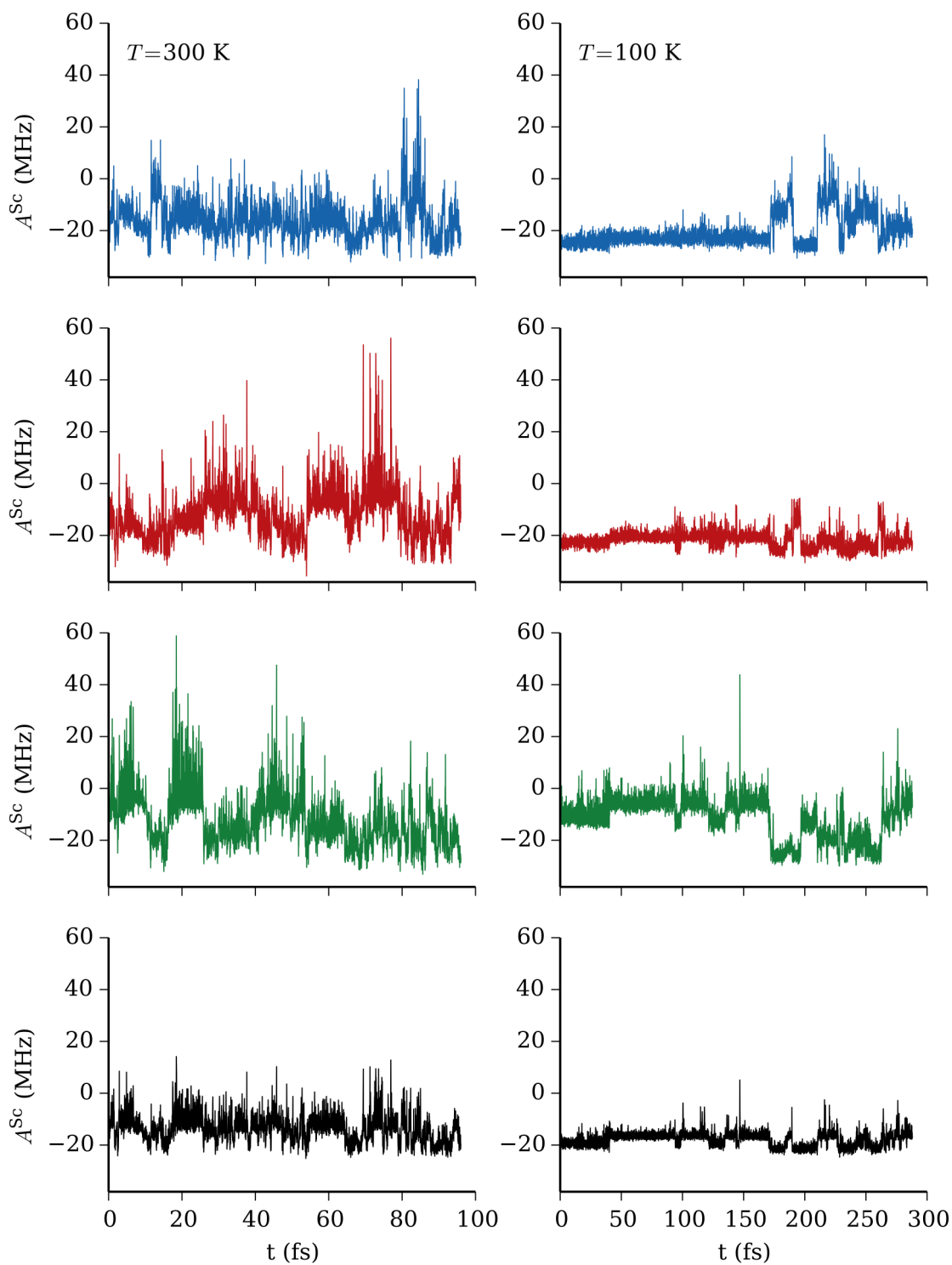


Figure S2: Isotropic hyperfine coupling constants of the three  $^{45}\text{Sc}$  nuclei (blue, red and green lines), and their mean value (black line), during the simulations at  $T = 300$  K (left panel) and 100 K (right).

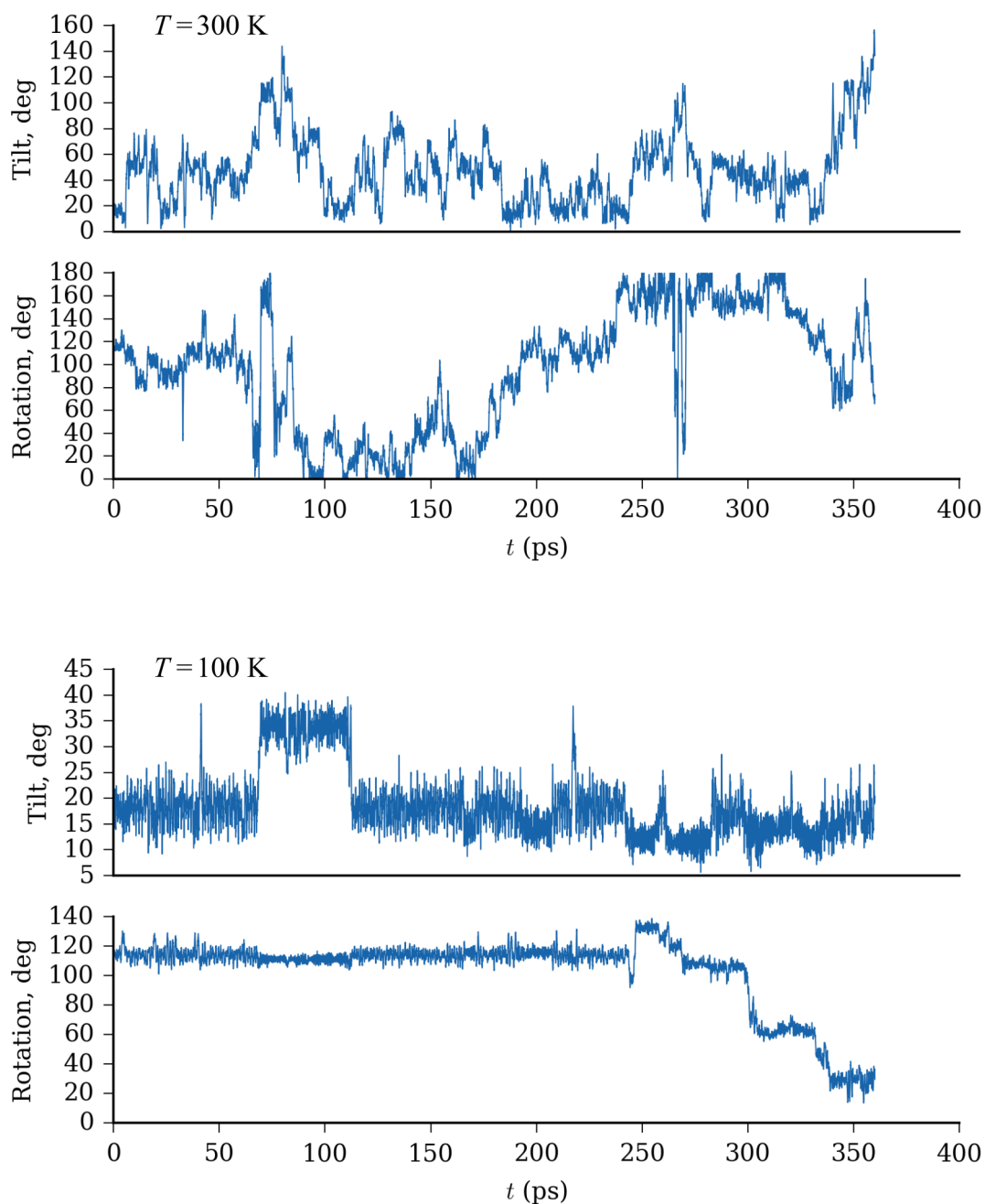


Figure S3: Relative tilt (angle between plane normals) and rotation in degrees between the plane formed by  $\text{Sc}_3$  and the plane formed by the reference carbons of the cage (see Figure S5), at  $T = 300$  K (top) and 100 K (bottom).

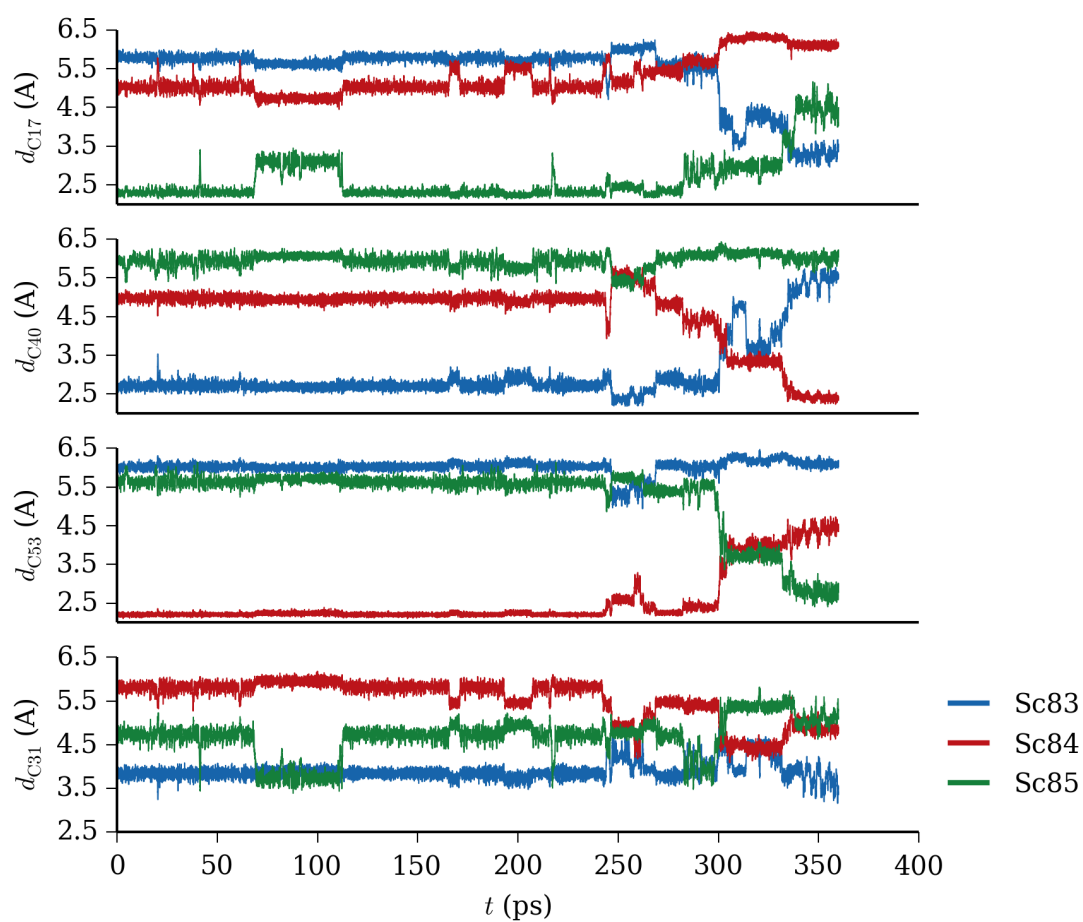


Figure S4: Distances between the scandium atoms and the reference carbons (see Figure S5) of the cage, at  $T = 100$  K.

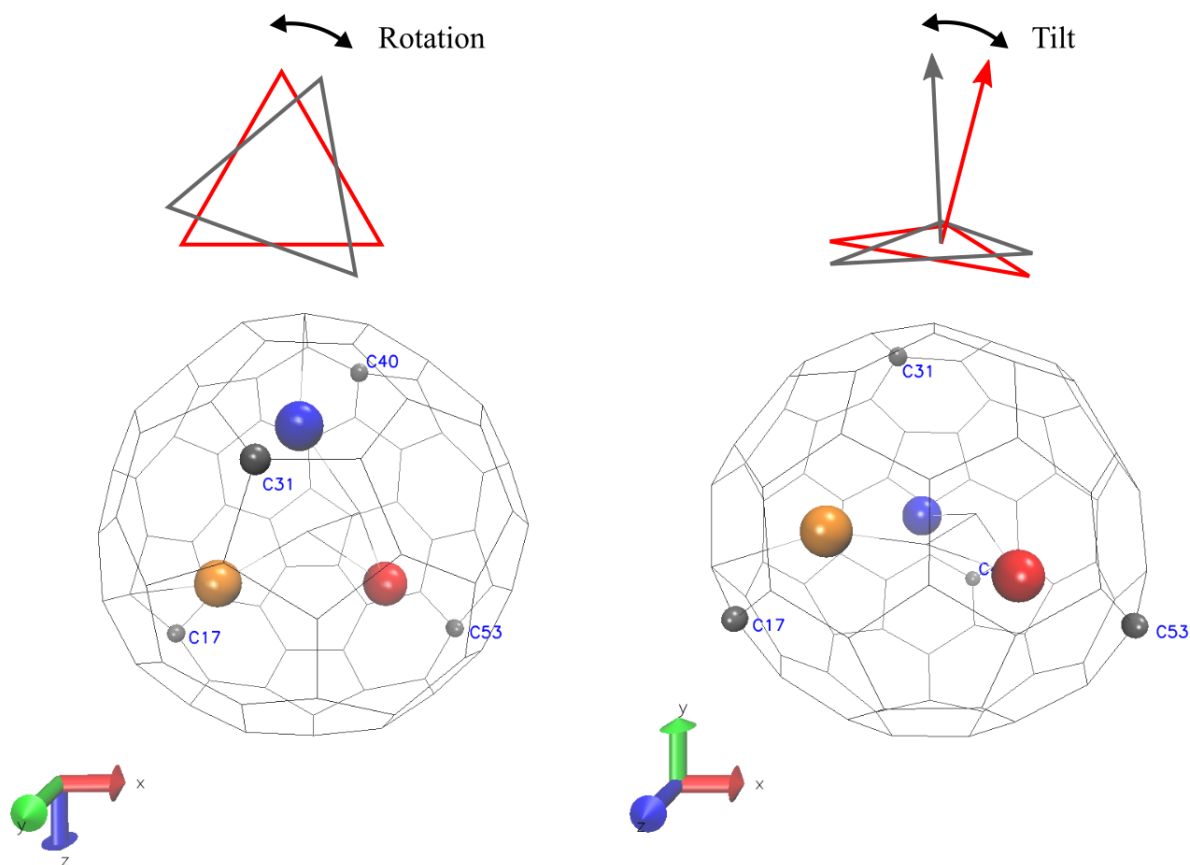


Figure S5: Reference carbon atoms used in the distance and angle plots. C17, C40 and C53 form a plane roughly along one 6-ring belt of the cage, while C31 is at the “top” of the cage relative to that plane. The tilt of the  $Sc_3$  plane relative to the C17–C40–C53 plane is defined as the angle between the normal vectors of the two planes. The relative rotation of the planes is defined as the angle between two vectors, one of which is on the C17–C40–C53 plane (*e.g.*, a vector from one atom to the midpoint between the two other atoms) and the other is a projection to that plane of a vector lying on the  $Sc_3$  plane.



Figure S6: Graphical representation of the shape and orientation of the  $\mathbf{A}$  tensors of each scandium, as viewed from the front of the  $\text{Sc}_3$  moiety (left picture) or top (right), averaged over the full trajectory at  $T = 100$  K. The ellipsoids are drawn with each axis corresponding to one principal value of the corresponding tensor. The scaling is the same for all nuclei, but chosen for visual purposes only.



Figure S7: Graphical representation of the shape and orientation of the  $\mathbf{A}$  tensors of each scandium, as viewed from the front of the  $\text{Sc}_3$  moiety (left picture) or top (right), averaged over the first 5000 calculations (the part of trajectory before  $\text{Sc}_3$  “jumps”) at  $T = 100$  K. The ellipsoids are drawn with each axis corresponding to one principal value of the corresponding tensor. The scaling is the same for all nuclei, but chosen for visual purposes only.

## 2 Computational details

The studied system consists of a  $\text{C}_{80}$  carbon cage enclosing three scandium metal atoms and a carbon dimer, denoted  $\text{Sc}_3\text{C}_2@\text{C}_{80}$ , with zero charge and

doublet electronic state (*i.e.*, spin multiplicity  $2S + 1 = 2$ ,  $S = 1/2$ ). The scandium trimer forms a not-quite-equilateral triangle, where two scandiums remain practically identical during the simulations, whereas the third one is inequivalent to them, due to the orientation of the carbide  $C_2$  unit that librates towards the non-identical scandium.

Molecular dynamics trajectories were calculated with density functional theory (DFT), using the BLYP functional [3, 4] as implemented in the CP2K [5] software package version 2.4 (at 300 K) and 2.5 (100 K). A cubic simulation cell with 12 Å long edges and a timestep of 2 fs was used in the simulations, along with a cutoff energy of 600 Ry and self-consistent field (SCF) convergence threshold of  $10^{-6}$ . The  $^{45}\text{Sc}$  ( $^{12}\text{C}$ ) core electrons were described using the norm-conserving GTH-BLYP-q11 (GTH-BLYP-q4) pseudopotential [6–8], and valence electrons with Gaussian DZV-GTH-PADE [9] (DZVP-GTH-BLYP [10]) basis sets optimised for the GTH pseudopotentials.

The 300 K trajectory was started from a geometry-optimised structure of the neutral isomer 2a reported by Taubert *et al.* [2]. The full trajectory consists of three parts: an initial microcanonical  $NVE$  simulation (duration 87.4 ps), an equilibrating, canonical  $NVT$  simulation (172.6 ps) with a canonical sampling/velocity rescaling (CSVR) [11] thermostat enabled, and a final microcanonical  $NVE$  simulation (100.0 ps) from which the property calculation snapshots were extracted. In the  $NVT$  simulation, the time constants of 100 fs (most of the region) and 1 fs were used for the thermostat, with little difference in the results. Figure S8 shows the temperature during the production  $NVE$  part of the 300 K simulation.

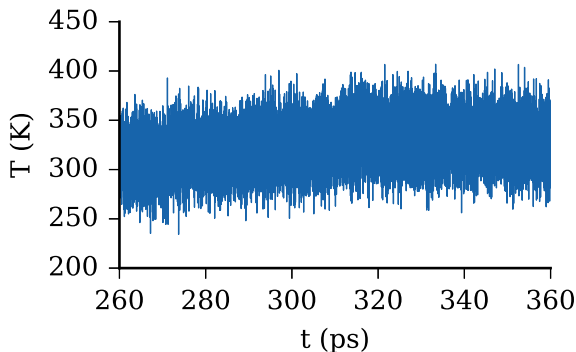


Figure S8: Temperature of the production  $NVE$  part of the 300 K MD simulation.

The 100 K trajectory was started from the same equilibrium geometry as the high-temperature trajectory, and consists of two parts: an initial canonical  $NVT$  trajectory (20 ps) with the CSVR thermostat enabled, and using 1 fs and 100 fs time constant regions, followed by a microcanonical  $NVE$  simulation (340 ps), from which the property calculation snapshots were ex-

tracted. Figure S9 shows the temperature during the production *NVE* part of the 100 K simulation.

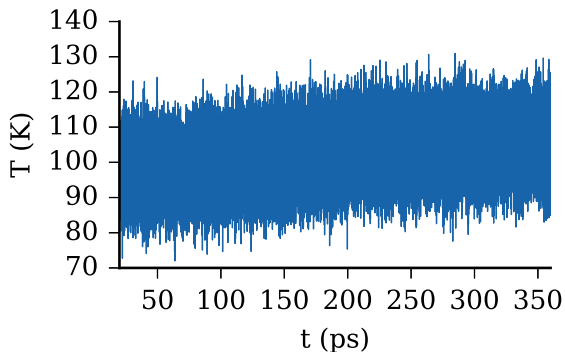


Figure S9: Temperature of the production *NVE* part of the 100 K MD simulation.

The electron paramagnetic resonance (EPR) parameters,  $g$  and hyperfine ( $\mathbf{A}$ ) tensors for each scandium were calculated using snapshot geometries extracted from the MD trajectories at constant intervals of 8 fs at 300 K (a total of 12000 snapshots), and 32 fs (a total of 9000 snapshots) at 100 K. The snapshots were selected starting from the last step of each trajectory towards the beginning, thus using the best-equilibrated part of the micro-canonical trajectory. The EPR parameters were calculated for each snapshot geometry with the Orca program system [12–14] version 3.0.3, using the resolution of the identity (RI) approximation [15] and the PBE functional [16, 17]. The grid and integration accuracy parameters were set to 7, and SCF convergence to “tight”. An uncontracted, completeness-optimised Gaussian basis set (dubbed co-r, 21s12p10d2f, *vide infra*) was used for scandium, while Def2-SVP and Def2-QZVPP [18, 19] basis sets were employed for cage and C<sub>2</sub> carbons, respectively.

Simulations of the EPR spectra were calculated with the EasySpin toolbox version 5.1.7 [20] on MATLAB R2015b [21]. The  $g$  and  $\mathbf{A}^{\text{Sc}}$  tensors used in the simulations are listed in Tables S1 and S2. In simulations based on isotropic constants, the  $g$ - and  $A$ -values of Table S3 were used. The experiment-related simulation settings, which were not available from first-principles calculations, were gathered from Ref. 1, to produce comparable figures. The X-band microwave frequency was not specified in the reference, and hence the value 9.385 MHz from the EasySpin documentation was used. High-temperature (300 K) simulations were run with the “garlic” program of EasySpin, applying Lorentzian broadening with full width at half maximum (FWHM) of 0.178 mT. Low-temperature (100 K) simulations were run with the solid-state “pepper” program of EasySpin, with the second-order perturbation theory approximation and Lorentzian broadening with FWHM of 0.6 mT. No Gaussian broadening was applied. The direct matrix-diagonalization

method was not applicable for this system due to very high resource requirements.

## 2.1 Completeness-optimised basis set for Sc

The co-r basis set shown in Table S4 was optimised using Kruunuhaka 2.0.1 basis set tool kit [22] by following the isotropic values of the  $g$  and  $\mathbf{A}^{\text{Sc}}$  tensors, as well as the  $A_{33}$  element of the SD contribution to the  $\mathbf{A}$  tensor, as calculated using Orca version 2.8 in a small  $\text{ScH}_2$  test system with the OLYP [23] functional and the RI approximation, setting the grid and integration accuracy to 7.

Table S4: Gaussian exponents of the completeness-optimised, uncontracted 21s12p10d2f basis set for scandium.

s	p	d	f
40238445.	2880.2919	626.53701	2.7179697
15582491.	1163.3533	232.03955	0.21356169
5601176.1	435.67808	83.123739	
1790589.7	161.81055	30.375595	
672553.42	57.892302	10.687894	
233927.39	20.042841	3.6495037	
77153.397	7.7789602	1.3569478	
23754.441	2.7506261	0.48991826	
7590.6403	1.0139505	0.17798017	
2345.3225	0.35374221	0.65559727E-01	
957.09586	0.13879297		
279.65475	0.56359098E-01		
105.05810			
40.461758			
12.087544			
3.3285515			
1.3642222			
0.39733190			
0.12672184			
0.51834597E-01			
0.20287268E-01			

## 2.2 Eckart frame of $\text{Sc}_3$

For comparison and averaging anisotropic properties between differently oriented snapshots, an in-house built program was used to transform the calculated  $g$  and  $\mathbf{A}^{\text{Sc}}$  tensors from the laboratory frame to the Eckart frame [24, 25] of the  $\text{Sc}_3$  subsystem. The equilibrium geometry used in the transformation was based on the structure that the MD simulations were started

from. To ensure that it is consistent with the MD simulations, a geometry optimization was performed with CP2K using the same functional and SCF settings as in the MD simulations, which resulted in almost no changes in the geometry, with differences between the old and new Sc positions being 0.036 and 0.049 Å (larger for the inequivalent scandium). The equilibrium structure is released as a separate Supporting Information file.

### 2.3 Movement of C<sub>2</sub>

The C<sub>2</sub> unit librates inside the Sc<sub>3</sub> triangle during the simulated trajectories. The movement is faster at 300 K, whereas at 100 K it is slower and, to some extent, it is possible to distinguish the two isomers 1a (C<sub>2</sub> perpendicular to the Sc<sub>3</sub> plane) and 2a (in the Sc<sub>3</sub> plane), found in Ref. 2. Despite the occasional perpendicular orientation, the libration mainly takes place towards one distinct scandium atom, and preserves the roles of the scandium atoms during the calculated trajectory. At 300 K, the dynamical motion of the system averages the scandium atoms effectively equivalent.

## References

- [1] J. Rahmer, L. Dunsch, H. Dorn, J. Mende and M. Mehring, *Magn. Reson. Chem.*, 2005, **43**, S192–S198.
- [2] S. Taubert, M. Straka, T. O. Pennanen, D. Sundholm and J. Vaara, *Phys. Chem. Chem. Phys.*, 2008, **10**, 7158–7168.
- [3] A. D. Becke, *Phys. Rev. A*, 1988, **38**, 3098–3100.
- [4] C. Lee, W. Yang and R. G. Parr, *Phys. Rev. B*, 1988, **37**, 785–789.
- [5] J. VandeVondele, M. Krack, F. Mohamed, M. Parrinello, T. Chassaing and J. Hutter, *Comput. Phys. Commun.*, 2005, **167**, 103–128.
- [6] S. Goedecker, M. Teter and J. Hutter, *Phys. Rev. B*, 1996, **54**, 1703–1710.
- [7] C. Hartwigsen, S. Goedecker and J. Hutter, *Phys. Rev. B*, 1998, **58**, 3641–3662.
- [8] M. Krack, *Theor. Chem. Acc.*, 2005, **114**, 145–152.
- [9] R. Pou-Amérigo, M. Merchán, I. Nebot-Gil, P.-O. Widmark and B. O. Roos, *Theor. Chim. Acta*, 1995, **92**, 149–181.
- [10] P.-O. Widmark, P.-Å. Malmqvist and B. O. Roos, *Theor. Chim. Acta*, 1990, **77**, 291–306.

- [11] G. Bussi, D. Donadio and M. Parrinello, *J. Chem. Phys.*, 2007, **126**, 014101.
- [12] F. Neese, *Wiley Interdiscip. Rev.: Comput. Mol. Sci.*, 2012, **2**, 73–78.
- [13] F. Neese, *ORCA: An Ab Initio, DFT and Semiempirical Electronic Structure Package*, 2016, Version 3.0.3, Department of Molecular Theory and Spectroscopy, Max Planck Institute for Chemical Energy Conversion, D-45470 Mülheim/Ruhr, Germany.
- [14] E. F. Valeev, *A Library for the Evaluation of Molecular Integrals of Many-body Operators over Gaussian Functions*, <http://libint.valeev.net>, 2014.
- [15] K. Eichkorn, O. Treutler, H. Öhm, M. Häser and R. Ahlrichs, *Chem. Phys. Letters*, 1995, **240**, 283–290. Erratum *Chem. Phys. Letters*, 1995, **242**, 652–660.
- [16] J. P. Perdew, K. Burke and M. Ernzerhof, *Phys. Rev. Lett.*, 1996, **77**, 3865–3868.
- [17] J. P. Perdew, K. Burke and M. Ernzerhof, *Phys. Rev. Lett.*, 1997, **78**, 1396–1396.
- [18] F. Weigend and R. Ahlrichs, *Phys. Chem. Chem. Phys.*, 2005, **7**, 3297–3305.
- [19] F. Weigend, *Phys. Chem. Chem. Phys.*, 2006, **8**, 1057–1065.
- [20] S. Stoll and A. Schweiger, *J. Magn. Reson.*, 2006, **178**, 42–55.
- [21] The MathWorks Inc.; MATLAB R2015b, Natick, Massachusetts, 2015.
- [22] P. Manninen and J. Lehtola, *Kruunuhaka basis set tool kit, Release 2.0*, <http://www.chem.helsinki.fi/~manninen/kruunuhaka>, 2011.
- [23] N. C. Handy and A. J. Cohen, *Mol. Phys.*, 2001, **99**, 403–412.
- [24] C. Eckart, *Phys. Rev.*, 1935, **47**, 552–558.
- [25] T. S. Pennanen, J. Vaara, P. Lantto, A. J. Sillanpää, K. Laasonen and J. Jokisaari, *J. Am. Chem. Soc.*, 2004, **126**, 11093–11102.